# Deferasirox loaded on fumed silica nanoparticles used in cancer treatment


| | |
|---|---|
| Journal: | *New Journal of Chemistry* |
| Manuscript ID | NJ-ART-10-2015-002790.R1 |
| Article Type: | Paper |
| Date Submitted by the Author: | 11-Jan-2016 |



| | |
|---|---|
| Complete List of Authors: | Taghavi, Faezeh; Ferdowsi University of Mashhad, Chemistry<br>Gholizadeh, Mostafa; Ferdowsi university of Mashhad, Chemistry Mashhad, Iran, Islamic Republic of, chemistry<br>Saljooghi, Amir Shokooh; Ferdowsi University of Mashhad, Chemistry |

RSC

Cite this: DOI: 10.1039/c0xx00000x

ARTICLE TYPE

www.rsc.org/xxxxxx

# Deferasirox loaded on fumed silica nanoparticles used in cancer treatment

**Faezeh Taghavi, Mostafa Gholizadeh, Amir Sh. Saljooghi***

***Received (in XXX, XXX) Xth XXXXXXXXX 20XX, Accepted Xth XXXXXXXXX 20XX***
**DOI: 10.1039/b000000x**

The present study has demonstrated paradigm of successful *in vitro* drug delivery systems using Fumed Silica Nanoparticles (FSNPs) as a scaffold. The surface of FSNPs was first coated with (3-aminopropyl)trimethoxysilane (APTMS) by a silanization reaction and then was linked with deferasirox via the reaction between $–NH_2$ and –COOH to form a well-dispersed surface functionalized biocompatible FSNPs. The obtained nanoparticles were thoroughly characterized by various spectroscopic and microscopic methods such as Fourier Transform Infrared Spectroscopy (FT-IR), Thermo Gravimetric Analysis (TGA) and Brunauer, Emmett and Teller (BET) surface area analysis. The morphology of these structures investigated by Scanning Electron Microscopy (SEM). The cytotoxicity of these compounds were screened for antitumor activity against MCF-7, MDA-MB-231, HeLa, HT-29, Neuro-2a, L929 cell lines and cisplatin used as a comparative standard by MTT assay. Our results presented herein provide experimental evidence that fumed silica nanoparticles loaded with deferasirox induce apoptosis in cancer cell lines. Our flow cytometry results confirm that, investigated compound showed a high population of apoptotic cell (55.20%) and 1.2-fold higher than cisplatin (45.15%) at the same concentration and could induce apoptosis of human breast cancer cell lines (MDA-MB-231).

*Corresponding Author: Amir. Shokooh Saljooghi, Ferdowsi University of Mashhad, Azadi Square, Mashhad, Iran. Postcode: 91735-654, Email: saljooghi@um.ac.ir

RSC

Cite this: DOI: 10.1039/c0xx00000x

www.rsc.org/xxxxxx

ARTICLE TYPE

## 1. Introduction

In recent years, Silica nanoparticles have confirmed to be a valuable material for biomedical research and they have attracted worldwide attention due to their easy preparation and their wide uses in various industrial applications, such as catalysis,[1] pigments, [2] pharmacy,[3] electronic[4] and thin film substrates,[5] electronic and thermal insulators,[6] and humidity sensors.[7] There are five types of silica-based materials used as drug delivery systems: 1) fumed silica nanoparticles,[8] 2) silica based xerogels,[9-13] 3) ordered mesoporous silica based materials,[14-18] 4) mesoporous silica spheres,[19-25] and 5) natural silica materials e.g. diatoms.[26-28] Because of the high surface area that provides good solubilisation properties in aqueous environment, fumed silica nanoparticles have been investigated as vehicles for accelerating the speed and the amount of dissolution of drugs that are poor to be solved in water.[29-30] Fumed silica is widely used for therapeutic applications, and their silanol containing surface can be functionalized, allowing better control over the drug release which depends on the chemical nature of the functional group attached to the surface.[31]

Coating the silica nanoparticles with amino groups leads to a large number of new applications, such as drug delivery,[32] gene delivery,[33] plasmid DNA transport,[34] capture and release of bacteriophage viruses,[35] and synthesis of silica polypeptide composite particles.[36-37]

Silanes are linked through the formation of a Si-O-Si bond between the surface and the silanol groups. Furthermore, this covalent attachment, a broad spectrum of available chemical functionalities at the other functional end of the silane molecules allow flexible adaptation of the surface for various applications. In particular, 3-(aminopropyl)trimethoxysilane (APTMS) has been broadly used because of its amino terminal group,[38-41] which makes APTMS especially attractive for biological purposes such as drug delivery. Terminal amino group is capable of a position for reacting with functional end of drugs or other molecules. This article describes modified silica with 4-[3,5-Bis(2-hydroxyphenyl)-1,2,4-triazol-1-yl]benzoic acid (Deferasirox) in anticancer studies. The deferasirox was covalently bound to 3-(aminopropyl)trimethoxysilane (APTMS) assembled on the particle surface through amidation between the carboxylic acid end groups on deferasirox and the pendant amine groups on the capping linker. At last, some investigations about other nanoparticles confirmed that drug cleaved from the nanoparticles inside cells.[42] The synthesis of deferasirox (4-[3, 5-bis(2-hydroxyphenyl)-1,2,4-triazol-1-yl]-benzoic acid, DFX or ICL670) was first reported in 1999.[43] In 2005, deferasirox became the first FDA approved oral alternative for treatment of iron overload and was subsequently approved in the EU in 2006.[44] It is a tridentate chelator with high selectivity for $Fe^{3+}$, and its $NO_2$ donation arises from one triazole nitrogen and two phenolate oxygen donors.[45]

This iron chelator is used for treatment of iron overload in the certain types of anemia such as $\beta$-thalassemia and treatment of other toxic metal overload.[46-47] In recent years, the potential for iron chelators in the treatment of cancer has emerged. "This reflects the fact that cancer cells typically require more iron than normal cells to mediate their generally rapid DNA synthesis and growth".[48] The aim of the present study was show the potential efficiency of antitumor activity of deferasirox loaded on fumed silica via an APTMS as a spacer.

## 2. Experimental

### 2.1. Chemicals

All solvents purchased from Merck. 4-Hydrazino-benzoic acid, triethyl amine ($NEt_3$) and 2-(2-Hydroxyphenyl)-4H-3, 1-benzoxazin-4-one without further purification, 1-ethyl-3-[3-dimethylaminopropyl] carbodiimide hydrochloride (EDC) and 7-Hydroxy benztriazole hydrate (HOBt) were purchased from Fluka (Germany). RPMI-1640 medium, Dulbecco's modified Eagle's medium (DMEM) and fetal bovine serum (FBS) were purchased from GIBCO (Gaithersburg, USA). Penicillin and streptomycin were purchased from Biochrom AG (Berlin, Germany). MTT (3-(4,5-dimethylthiazol-2-yl)-2,5-diphenyltetrazolium bromide, a yellow tetrazole) was purchased from Sigma Co., Ltd. Cisplatin was purchased from Sigma Aldrich.

### 2.2. Apparatus

NMR spectra were recorded on Avance Brucker-400 MHz spectrometers. All Chemical shifts in NMR experiments are reported as ppm and were referenced to residual solvent. Chemical shifts are reported in parts per million and the signals are quoted as s (singlet), br (broad), d (doublet) and m (multiplet). FT-IR spectra were recorded on AVATAR-370-FTIR Thermo Nicolet. All Mass spectra were scanned on a Varian Mat CH-7 at 70 eV. Reaction was monitored by TLC using silica gel plates and the products were identified by comparison of their spectra and physical data with those of the authentic samples. Melting points were measured on an Electrothermal 9100 apparatus. The Scanning Electron Microscopy (SEM, EDS) images were taken on a Zeiss LEO 1450 VP/35Kv, Germany. Thermo Gravimetric Analysis (TGA) was carried out using thermogravimetric analyzer TGA-50 (Shimadzu Japan) instruments. Elemental analysis was carried out using CHNS (O) Analyzer Model FLASH EA 1112 series made by Thermo Finnigan.

### 2.3. Synthesis of 4-[3, 5-Bis (2-hydroxyphenyl)-1, 2, 4-triazol-1-yl] benzoic acid (deferasirox)

2-(2-Hydroxyphenyl)-4H-3,1-benzoxazin-4-one was prepared according to the previous reported procedure with a little modifications.[49-50] 4-Hydrazino-benzoic acid (11.5 mmol, 1.75 g) and $Et_3N$ (11.5 mmol, 1.16 g) were dissolved in boiling EtOH (80 mL). Then, 2-(2-Hydroxyphenyl)-4H-3,1-benzoxazin-4-one (10.45 mmol, 2.50 g) was added to the clear solution, and the reaction mixture was refluxed for an additional 2 h. After the completion of the reaction, the solution was cooled to room temperature, and water was added until the first sign of precipitation was observed. The mixture was concentrated to a total volume of 50% under reduced pressure and aqueous 6M HCl (40 mL) was added. The resulting solid was filtered, washed with water and dried for 24 h in vacuo (3.11 g, Yield = 80%).

Yellow powder; (3.11 g, Yield = 80%); m.p. 264-266 ˚C IR (KBr) ν: 3317, 2540, 1680 (C=O), 1607, 1517, 1495, 1431, 1351, 1221, 988, 752 $cm^{-1}$; $^1H$ NMR ($C_3H_6O$-$d_6$ 400 MHz): δ 7.00 (s, 1H), 7.01-7.04 (m, 3H), 7.39 (m, 2H), 7.48 (d, 1H), 7.53 (d, 2H), 8.15 (d, 2H), 8.19 (d, 1H) 10.00 (s, OH), 10.78 (s, OH ) ppm; $^{13}C$ NMR ($C_3H_6O$-$d_6$, 75 MHz): δ 113.7, 113.9, 116.6 (CH), 117.0 (CH), 119.5 (CH), 119.8 (CH), 124.0 (2CH), 126.9 (CH), 130.4 (2CH), 130.5, 130.7 (CH), 131.4 (CH), 132.6, 141.9 (CH), 152.1, 155.6, 156.4, 160.4, 165.7 (C=O) ppm; M.S. (70 eV) m/z (%): 374 (M+, 100); Anal. Calc. for $C_{21}H_{15}N_3O_4$:.C, 67.56; H, 4.05; N, 11.25. Found C, 67, 76; H, 3.85; N, 11.14.

### 2.4. Loading of deferasirox on fumed silica nanoparticles

In order to bind the silica nanoparticles (NPs) to deferasirox, at first, the nanoparticles are treated with 3-(aminopropyl)trimethoxysilane (APTMS). In a subsequent reaction, the silanol groups condensate with the hydroxyl groups on the NPs' surface to form Si-O-Si covalent bonds. This method introduces the NPs surface of the amino group that is essential to create an amide bond with the activated carboxylic group of deferasirox.

Fumed silica (particle size: 200 nm) was chemically modified as follows: first, it was activated at 150 ºC under Vacuum (0.1 Pa) for 5 h. 3-(aminopropyl)trimethoxysilane (32 ml) was dissolved in 100 ml toluene and it was added to activate silica (31.9 g). This mixture was refluxed with stirring for 8 h; the product was filtered and washed with toluene (soxhlet extraction for 24 h) and finally, it was dried at 40-50 ºC for 6 h. Then, deferasirox (4.2 mmol) was dissolved in 100 ml of toluene and then was added to 1.1 g of the previous sample in present of EDC (50mg)/ HOBt (40 mg) compounds to activate the carboxylate groups of deferasirox for amide bond formation. EDC/HOBt (also NHS) cross linking leads to amide bond formation between activated carboxyl groups and amine groups. This mixture was refluxed under stirring for 24 h and was filtered and washed with 100 ml of dry toluene (soxhlet extraction) for 24 h. The solid product was dried at room temperature under vaccum and abbreviated by FS-APTMS-DFX. The synthesis of fumed silica nanoparticles loaded with deferasirox was carried out according to the steps showed in Scheme 1.

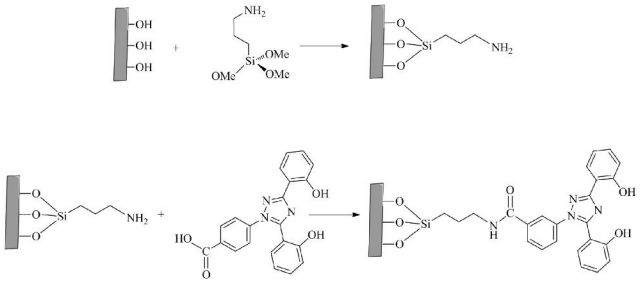

**Scheme 1** Genaral synthesis of FS-APTMS-DFX

### 2.5. Characterization of Silica Nanoparticles Loaded with Deferasirox

The composition and pore structures were thoroughly studied with various spectroscopic and microscopic methods such as FT-IR, TGA, SEM-EDS and BET techniques.

Fig. 1 shows the FT-IR spectra of Fumed Silica (FS), FS-APTMS, FS-APTMS-DFX. Fig. 1 (a) demonstrate the peak at 1113 $cm^{-1}$ corresponding to the Si-O-Si stretching modes of silica gel and a broad adsorption peak at 3400 $cm^{-1}$ belonging to Si-OH groups. Fig. 1 (b) indicates FT-IR spectrum of FS-APTMS; the peaks at 1034-1123, 1388 and 1560 $cm^{-1}$ are allocated to Si-O-Si (asymmetric stretching), C-N (stretching vibration) and N-H (bending), respectively. Furthermore, several bands with medium intensity in 2872-2929 and 3436 $cm^{-1}$ are attributed to C-H stretching of propyl group and N-H stretching mode. In the FT-IR spectrum of FS-APTMS-DFX, new bands are observed at 1466, 1565 and 1644 $cm^{-1}$ due to the aromatic C=C stretch and C=N stretch of deferasirox. C=O stretch of amide group appears at 1711 $cm^{-1}$. Moreover, presence of broad absorption peaks in 3039-3299 regions demonstrates the O-H groups of deferasirox and N-H stretching band of amide (Fig. 1 (c)). Observed bands confirmed that immobilization of organic molecule to the silica surface has been accomplished successfully.

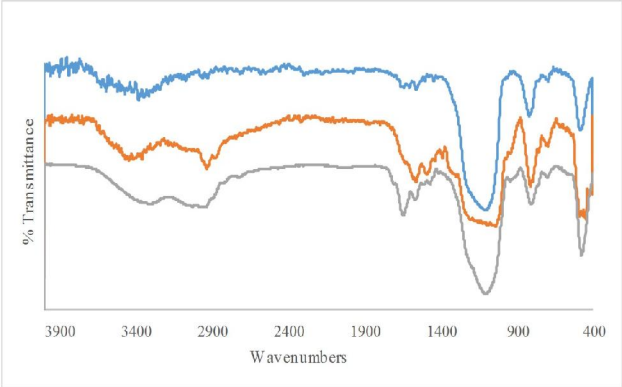


**Fig. 1** (a) Infrared spectra of Fumed silica (FS), (b) silica modified with 3-(aminopropyl)trimethoxysilane (FS-APTMS) and (c) Defrasirox anchored on FS-APTMS (FS-APTMS-DFX).

TGA of FS-APTMS shows weight loss below 150 $^0$C is due to the removal of physisorbed water or the water that obtained from the condensation of hydroxyl groups. Moreover, the main weight change (about 14%) in the temperature ranges of 150-600 $^0$C was observed attributed to the decomposition of the amino propyl group on the surface. In the case of FS-APTMS-DFX, increase of weight loss about 31% was found in the temperature between

200-600 $^0$C. Thus, these results confirmed the successful immobilization of the organic structure on the silica.

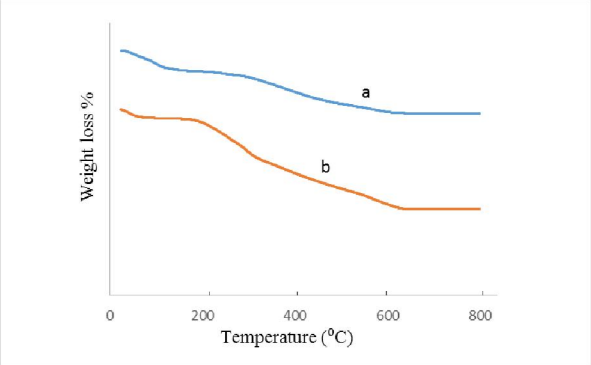


**Fig. 2** TGA of: (a) silica modified with 3-(aminopropyl)trimethoxysilane (FS-APTMS) and (b) Defrasirox anchored on FS-APTMS (FS-APTMS-DFX).

Scanning Electron Microscopy (SEM) was used to observe the morphology of fumed silica nanoparticles before and after deferasirox loading. Using scanning electron microscopy, it is possible to obtain information about the surface properties of the nanoadsorbents (Fig. 3).

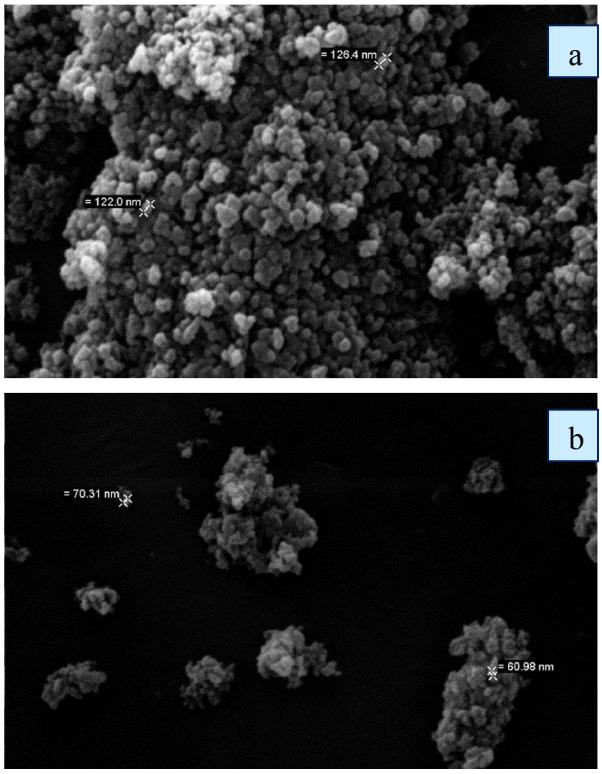


**Fig. 3** SEM of: (a) silica modified with 3-(aminopropyl)trimethoxysilane (FS-APTMS) and (b) Deferasirox anchored on FS-APTMS (FS-APTMS-DFX).

In accordance with the scanning electron microscopy it can be postulated that the nanoparticles were in uniform spherical shape. The energy dispersive spectrum (EDS) indicated the presence of Si, N, C and O elements (Fig. 4). This analysis confirms that fumed silica nanoparticles were loaded by organic structures.

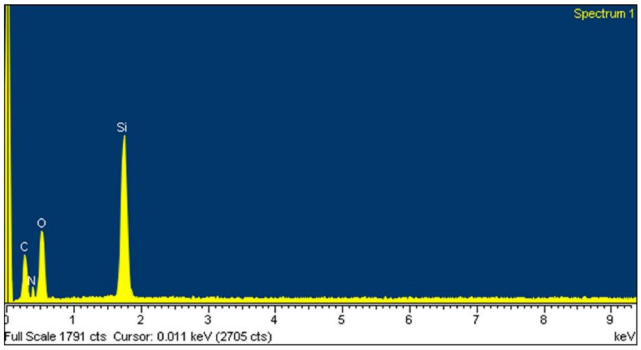


**Fig. 4** The EDS spectrum of Deferasirox anchored on FS-APTMS (FS-APTMS-DFX)

The particle size of silica nanoparticles were found by DLS analysis with polydispersity index (PDI) < 0.2, indicating a narrow size distribution.

Table 1 gives the specific surface area and the mean pore diameter data of the fumed silica (FS), silica modified with 3-(aminopropyl)trimethoxysilane (FS-APTMS) and Deferasirox anchored on FS-APTMS (FS-APTMS-DFX). From the nitrogen adsorption-desorption isotherms and BET analysis the specific surface area of FS, FS-APTMS and FS-APTMS-DFX were calculated as 170 ± 5.1, 73.9 ± 3.2 and 53.4 ± 1.7 $m^2g^{-1}$ respectively.

**Table 1** Specific surface area and the mean pore diameter data of the FS, FS-APTMS and FS-APTMS-DFX

| Sample | $S_{BET}$ ($m^2g^{-1}$) | Mean pore diameter (nm) |
|---|---|---|
| FS | 170 ± 5.1 | 11.15 ± 0.37 |
| FS-APTMS | 73.9 ± 3.2 | 20.23 ± 0.71 |
| FS-APTMS-DFX | 53.4 ± 1.7 | 22.46 ± 0.67 |

## 3. Biological Studies

### 3.1. Cell Culture Methods

human breast cancer cells MCF-7 (ATCC HTB-22), MDA-MD-231 (ATCC HTB-26), human cervix epithelial carcinoma HeLa (ATCC CCL-2), human colon cancer cell line HT-29 (ATCC HTB-38), mouse neuroblastoma cell line Neuro-2a (ATCC CCL-131), mouse fibroblast L929 cell line (ATCC CCL-1) were obtained from the American Type Culture Collection (ATCC; Manassas, VA, USA) and cultured at 37 °C in a humidified atmosphere of 5% $CO_2$ in air. HeLa cells were cultured in Dulbecco's Modified Eagle's Medium (DMEM) with 0.1 mM nonessential amino acids, 2 mM-glutamine, 1.0 mM sodium pyruvate and 5% fetal bovine serum, at 37 °C in an atmosphere of 5% $CO_2$. Cells were plated in 96-well sterile plates at a density of $1\times10^4$ cells/well in 100 µL of medium and incubated for 24 h. Also, MCF-7, MDA-MD-231, HT-29 and cells Neuro-2a were cultured in Dulbecco's Modified Eagle's Medium (DMEM) containing 10% fetal bovine serum, 100 units/mL of penicillin and 100 µg/mL of streptomycin. L929 cells were cultured in RPMI-1640 containing 10% fetal bovine serum,

100 units/mL of penicillin and 100 µg/mL of streptomycin.

### 3.2. MTT Assay in Human Cancer Cell Lines

FS-APTMS-DFX was screened for antitumor activity against human breast cancer cells (MCF-7 and MDA-MD-231), human cervix epithelial carcinoma (HeLa), human colon cancer cell line (HT-29), and mouse neuroblastoma cell line (Neuro-2a), mouse fibroblast L929 cell line and cisplatin used as a comparative standard by MTT assay. Cell viability was evaluated by using a colorimetric method based on the tetrazolium salt MTT ([3-(4,5-dimethylthiazol-2-yl)-2,5-diphenyltetrazolium bromide]), which is reduced by living cells to yield purple formazan crystals. Cells were seeded in 96-well plates at a density of 2-5×$10^4$ cells of MCF-7, HeLa, HT-29, MDA-MD-231, Neuro-2a and L929 per well in 200 µL of culture medium and left to incubate overnight for optimal adherence. After careful removal of the medium, 200 µL of a dilution series of FS-APTMS-DFX in fresh medium were added and incubation was performed at 37 °C/5% $CO_2$ for 72 h. FS-APTMS-DFX was first solubilized in DMSO, diluted in medium and added to the cells in final concentrations between 20 nM and 200 µM. The percentage of DMSO in cell culture medium did not exceed 0.3%.[51] Cisplatin was first solubilized in saline and then was added at the same concentrations used for the other compounds. At the end of the incubation period, the investigated compound was removed and the cells were incubated with 200 µL of MTT solution (500 µg/ml). After 3–4 h at 37 °C/5% $CO_2$, the medium was removed and the purple formazan crystals were dissolved in 200 µL of DMSO by shaking. The cell viability was evaluated by measurement of the absorbance at 570 nm by using a STAT FAX-2100 microplate reader (Awareness Technology, Palm City, FL, USA). The cell viability calculated the division of the absorbance of each well by that of the control wells (cells treated with medium containing 0.3% DMSO). Each experiment was repeated at least three times and each point was determined in at least three replicates.

The amounts of $EC_{50}$ obtained using deferasirox concentration in nanoparticles as described by Buchman *et al*.[52] In this method, the total nitrogen in each stage obtained by elemental analysis. In following, we used Ninhydrin quantitative test to determination of primary amines before and after drug (deferasirox) loading on silica nanoparticles.

### 3.3. Apoptosis Assay for FS-APTMS-DFX by Flow Cytometry

Evaluation of apoptosis by flow cytometry is generally accomplished by methods that use annexin V-FITC as vital dye, which access phosphatidyl serine exposed to the external membrane at the beginning of this process. The differentiation between apoptotic and necrotic cells can be performed by simultaneous staining with Propidium Iodide (PI). Therefore, Annexin V-FITC was used as a marker of phosphatidyl serine exposure and PI as a marker for dead cells. This combination allows differentiation among early apoptotic cells (annexin V-positive, PI-negative), late apoptotic/necrotic cells (annexin V-positive, PI-positive), and viable cells (annexin V-negative, PI-negative).

Cells lines ($5×10^5$) were seeded and treated with the investigated compound FS-APTMS-DFX and incubated for 24 h at a concentration close to the $EC_{50}$ at 37 °C. Following treatment, the cells were harvested by trypsination and centrifugation at 1000 r.p.m. for 5 min. The supernatant was removed, and the cell pellet was washed in PBS followed by two washes in binding buffer (10 mM HEPES, 150 mM NaCl, 5 mM KCl,1.8 mM $CaCl_2$, 1 mM $MgCl_2$). The cells were incubated with an Annexin V/FITC antibody (5 ml in 100 ml binding buffer) and incubated at 4 °C for 15 min in the dark. Samples were washed in binding buffer, and the supernatant was discarded. The pellet re-suspension 490 ml binding buffer and 10 ml propidium iodide (10 mg $ml^{-1}$ in PBS) was added to the samples before analysis by flow cytometry. Flow cytometry was done by using Partec PAS flow cytometer (PartecGmbH, Germany) on FS-APTMS-DFX and cisplatin as a reference.

Also apoptosis was detected using an *in situ* cell death detection kit (Boehringer Mannheim Corp., Indianapolis, IN) as described by Narla *et al*. and Zhu *et al*.[53-54] Cells were incubated with DFX in 0.3% DMSO or 1:16-diluted plasma samples from DFX-treated mice for 48 h at 37 °C, and were fixed, permeabilized, incubated with the reaction mixture containing TdT- and FITC-conjugated dUTP, and counterstained with propidium iodide. Cells were transferred to slides and viewed with a confocal laser scanning microscope (Bio-Rad MRC 1024) mounted on a Nikon Eclipse E800 series upright microscope as reported previously Narla et al. and Zhu *et al*.

### 3.4. Statistical Analysis

$EC_{50}$ values expressed as mean ± standard deviation (SD) from at least three independent experiments. Statistical tests including one way ANOVA, Tukey multiple comparison or unpaired Student's *t*-tests were performed using SPSS, version 17 software. A *p* value of less than 0.05 was considered as significant.

**Table 2** Cytotoxic activity of FS-APTMS-DFX tested against MCF-7, HeLa, HT-29, MDA-MB-231, Neuro-2a cancer cell lines and L929 after 72 h continuous Exposure .

| $EC_{50}$ ± SD (µM) [a] | | | | | | |
|---|---|---|---|---|---|---|
| **Compound** | **MCF-7** | **HeLa** | **HT-29** | **MDA-MB-231** | **Neuro-2a** | **L929** |
| **FS** | 97.8± 8.3 | 147.5 ± 11.2 | 134.6 ± 11.3 | 105.2 ± 9.5 | 175.4 ± 12.9 | 235.2 ± 17.7 |
| **FS-APTMS** | 85.3 ± 7.9 | 102.1 ± 10.9 | 69.4 ± 8.3 | 85.7 ± 6.9 | 122.4 ± 9.8 | 135.2 ± 12.1 |
| **FS-PTMS-DFX** | 17.4 ± 3.66 | 35.9 ± 4.98 | 17.1 ± 2.68 | 8.52 ± 2.24 | 87.4 ± 9.53 | 241.3 ± 17.5 |
| **DFX** | 53.9 ± 6.1 | 38.2 ± 3.9 | 16.5 ± 3.62 | 39.9± 4.1 | 100.7 ± 9.4 | 102.3 ± 9.5 |
| **Cisplatin** | 5.94 ± 1.47 | 0.45 ± 0.13 | 19.3 ± 3.46 | 24.7 ± 4.71 | 103 ± 9.8 | 0.7 ± 0.2 |

[a] $EC_{50}$ The effective concentration at 50% of the total effect. The experiments were done in triplicate. Data were expressed as the mean of the triplicate. $EC_{50}$> 100 µM is considered to be inactive.[55]

## 4. Results and Discussion

In recent years, some studies confirmed the apparent association between excess iron and cancer, there is significant interest in the investigation and development of iron chelating drugs as anti-neoplastic agents.[56-57]"This reflects the fact that cancer cells typically require more iron than normal cells to mediate their generally rapid DNA synthesis and growth".[48]

Developments of organofunctionalized hybrid silica nanoparticles (SNs) materials technology applied to its manufacturing procedure adds a strong tool in molecular oncology to wrap up pre-existing anticancer drugs into nanoparticle formulations that alter the biodistribution, lower the side effects, minimize the toxic exposure to normal tissues while maximizing tumor uptake and penetration of the drug. Therefore, fumed silica nanoparticles (with oral and dermal delivery route), with particular emphasis on their role in cancer therapy was synthesized and used in biological model.

In this study, the potential of interesting iron chelator, deferasirox, that loaded on fumed silica nanoparticles as effective anticancer compound have been investigated *in vitro*. In order to gain this aim, the *in vitro* cytotoxiciy of FS-APTMS-DFX, FS-APTMS, FS and the free drug (DFX), against MCF-7, HeLa, HT-29, MDA-MB-231, Neuro-2a and L929 cell lines was determined by MTT-based assays (Table 2). For the free drug, FS-APTMS-DFX, FS-APTMS, FS and cisplatin we have measured the $EC_{50}$ values in all cell lines. Such measurements were done after 72 h of incubation and using concentrations of the compounds in the range 20 nM and 200 µM. The values determined for FS-APTMS-DFX spanned between 8.52 and 241.3 µM, while those found for the comparative standard ranged between 0.7 and 103 µM (Table 2). FS-APTMS-DFX exhibits the highest selectivity against MDA-MB-231 and HT-29. It is notable that FS-APTMS and FS is less cytotoxic than FS-APTMS-DFX against all cancer cell lines. Also DFX is less cytotoxic than FS-APTMS-DFX against all cancer cell lines except HT-29. FS-APTMS-DFX in the same range, is nearly three times more cytotoxic than cisplatin against MDA-MB-231 while it is five times more cytotoxic than DFX against this cell line. The cytotoxicity of free drug is the same as cisplatin and FS-APTMS-DFX against HT-29. Also, the FS, FS-APTMS and DFX are inactive against all cancer cell lines and L929 (except DFX against HT-29). The effect of synthesized compound on mouse fibroblast cell line (L929) was evaluated as control, simultaneously. Our results confirmed that the synthesized compound have not any cytotoxicity effects on L929.

In order to study in which way these compounds produced the cellular death (*i. e.* necrosis or apoptosis), studies of flow cytometry were performed on FS-APTMS-DFX and cisplatin as a reference. The results were shown in Table 3 and Fig. 5. Four areas in the diagrams stand for necrotic cells (Q1, left square on the top), late apoptosis or necrosis cells (Q2, right square on the top), live cells (Q3, left square at the bottom), apoptosis cells (Q4, right square at the bottom), respectively. As it can be seen in Table 3 and Fig. 5 investigated compound showed a high population of apoptotic cell (55.2%) and nearly 1.2-fold higher than cisplatin (45.15%) at the same concentration. The results demonstrated that the newly synthesized compound could induce apoptosis against MDA-MB-231 cancer cell line. But the proapoptotic property needs further investigation in order to understand the precise mechanism of action of these compounds much better and basic pre-clinical research is needed before they could be recommended for human administration.

**Table 3** Percentages of the cell death pathways observed by the flow cytometry assay.

| Treatment | % Vital cells | % Apoptotic cells | % Late apoptotic/necrotic cells | % Necrotic cells |
|---|---|---|---|---|
| Control | 98.1 | 0.43 | 0.94 | 0.53 |
| Cisplatin | 50.3 | 8.05 | 37.1 | 4.55 |
| FS-APTMS-DFX | 41.6 | 25.5 | 29.7 | 3.20 |

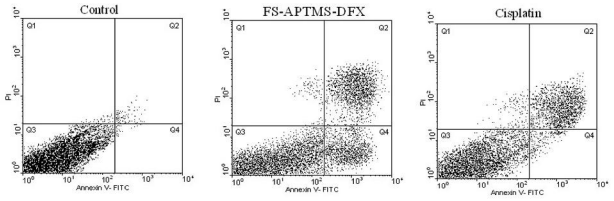


**Fig. 5** Flow cytometric results after the exposure of MDA-MB-231 cancer cells to investigated compound and cisplatin. Four areas in the diagrams represent four different cell states: necrotic cells (Q1), late apoptotic or necrotic cells (Q2), living cells (Q3) and apoptotic cells (Q4)

Also the FS-APTMS-DFX induced cell death was confirmed to be apoptotic using the TUNEL of exposed 3'-OH termini of DNA with dUTP-FITC. As shown in the confocal laser scanning microscopy images in Fig. 6, (FS-APTMS-DFX)-treated MDA-MB-231 breast cancer cells, examined for dUTP-FITC incorporation (*green fluorescence*) and propidium iodide counterstaining (*red fluorescence*), exhibited many apoptotic yellow nuclei (*superimposed green and red fluorescence*) at 24 h after treatment.

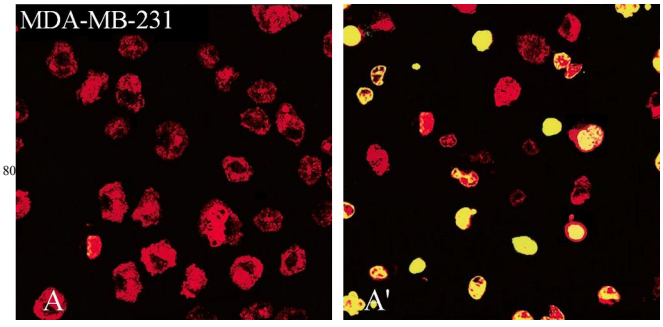


**Fig. 6** FS-APTMS-DFX induces apoptosis in breast cancer cells. MDA-MB-231 breast cancer (A, A') cells were incubated with 10 mM of FS-APTMS-DFX for 24 h, fixed, permeabilized

and visualized for DNA degradation in a TUNEL assay using dUTP-labeling. *Red fluorescence*, nuclei stained with propidium iodide. *Green or yellow* (*i.e., superimposed red and green*) *fluorescence*, apoptotic nuclei containing fragmented DNA. When compared with controls, treated with 0.3% DMSO (A), several of the cells incubated with FS-APTMS-DFX (A') exhibited apoptotic nuclei.

## 5. Conclusion

In summary, we investigate for the first time *in vitro* antitumor activity and antiproliferative effects of deferasirox (DFX) against some cancer cell lines. In this study, we used fumed silica nanoparticles (FS) as surface that drug was covalently bond to linker (APTMS) through formation of amid bond between the carboxylic acid end groups on deferasirox and the pendant amine groups of linker. Fumed silica nanoparticle can be donate some characteristics such as improved bioavailability, increasing resistance time in the body and etc. *In vitro*, the nanoparticles that loaded with anticancer drug were found to show a higher apoptosis-inducing effect in cancer cell lines than free drugs. These results are in agreement with previous reports. Deferasirox, despite its good cell permeability, it is practically insoluble in water, being classified as a Class II drug (poorly soluble, highly permeable) according to the Biopharmaceutics Classification System (BCS).[58] Also, due to its insolubility in water, the method advised to patients for taking the medicine orally is quite cumbersome.[59] Due to the high surface area that provides good solubilisation properties in aqueous environment, fumed silica nanoparticles have been investigated as vehicles for enhanced rate and extent of dissolution of poorly water soluble drugs. Fumed silica nanoparticles based solid dispersions have been demonstrated to enhance dissolution rate and extent *in vitro* and *in vivo* bioavailability of water insoluble drug.[60-61]

Furthermore, we used dense silica nanoparticles to accumulate drug concentration at the surface of cell monolayers; manipulations that increased complex concentration at the cell surface enhanced cytotoxic effect in cancer cell lines than free drugs.[62] We believe that the enhanced solubility and enhanced drug concentration at the surface of cancer cells, due to grafting deferasirox (DFX) to silica nanoparticles (FS-APTMS), caused that FS-APTMS-DFX show high cytotoxicity effects in Comparison to DFX. The cytotoxicity of this compound was screened for antitumor activity against some cell lines using cisplatin as a comparative standard by MTT assay and flow cytometry. The pharmacological results suggest that the fumed silica nanoparticles loaded with deferasirox is potent anticancer agent. Besides, the cytotoxicity of this compound is higher than free drug (DFX). The effect of synthesized compound on mouse fibroblast cell line (L929) was evaluated as control, simultaneously. Our results confirmed that the synthesized compound have not any cytotoxicity effects on mouse fibroblast cell line (L929). Furthermore, the FS-APTMS-DFX has been successfully used for bioimaging by using a confocal laser scanning microscope, which may be favorable for biological applications.

## Aknowledgement

Authors are grateful from Ferdowsi university of Mashhad, research council and Buali research institute, faculty of Pharmacy, Mashhad university of Medical Sciences for supporting this work.

## References

1. A. Fihri, D. Cha, M. Bouhrara, N. Almana and V. Polshettiwar, *Chem. Sus. Chem.,* 2012, **5**, 85–89.
2. J. Yuan, W. Xing, G. Gu and L. Wu, *Dyes. Pigments.,* 2008, **76**, 463-469.
3. S. Chattoraj, L. Shi and C. C. Sun, *J. Pharm. Sci.,* 2011, **100**, 4943-4952.
4. V. M. Gun'ko, Y. V. Zaulychnyy, B. I. Ilkiv, V. I. Zarko, Y. M. Nychiporuk, E. M. Pakhlov, Y. G. Ptushinskii, R. Leboda and J. Skubiszewska-Zięba, *Appl. Surf. Sci*., 2011, **258**, 1115-1125.
5. M. Bao, G. Zhu, L. Wang, M. Wang and C. Gao, *Desalination,* 2013, **309**, 261–266.
6. V. Lysenco, P.H. Roussel, B. Remaki, G. Delhomme, A. Dittmar and D. Arbier, *J. Porous. Mater*., 2000, **7**, 177–182.
7. D. Viegas, J. Goicoechea, J. L. Santos, F. M. Araújo, L. A. Ferreira, F. J. Arregui and I. R. Matias. *Sensors,* 2009, **9**, 519-527.
8. R. Chang K. Leonzio and M. M. A. Hussain, *Pharm. Dev. Technol.,* 1999, **4**, 85-89.
9. S. B. Nicoll, S. Radin, E. M. Santos, R. S. Tuan and P. Duchene*, Biomaterials*, 1997, **18**, 853-859.
10. P. Kortesuo, M. Ahola, M. Kangas, T. Leino, S. Laakso, L. Vuorilehto, A. Yli-Urpo, J. Kiesvaara and M. Marvola, *J. Control Release*, 2001, **76**, 227-238.
11. M. Ahola , P. Kortesuo, I. Kangasniemi, J. Kiesvaara and A. Yli-Urpo, *Int. J. Pharm*., 2000, **195**, 219-227.
12. H. Bottcher, P. Slowik and W. Sub, *J. Sol-Gel Sci. Technol*., 1998, **13**, 277–281.
13. M. S. Ahola , E. S. Sailynoja, M. H. Raitavuo, M. M. Vaahtio, J. A. Salonen and A. U.O.Yli-Urpo, *Biomaterials*, 2001, **22**, 2163-2170.
14. M. M. De Villiers, P. Aramwit and G. S. Kwon, Eds. *Nanotechnology in drug delivery*, Springer, AAPS Press: 2009.
15. D. Van, T. M. C. Guire and R. Langer*, Nat. Biotechnol.,* 2003, **21**, 1184-1191.
16. C. Wei, W. Wei, M. Morris, E. Kondo, M. Gorbounov and D. A. Tomalia*., Med. Clin. North Am*. 2007, **91**, 863-870.
17. M. Vallet-Regi, F. Balas, M. Colilla and M. Manzano, *Prog. Solid State Chem*., 2008, **36**,163-191.
18. M. Vallet-Regí, *Chem. Eur. J.*, 2006, **12**, 5934-5943.
19. K. K.Coti, M. E. Belowich, M. Liong,M. W. Ambrogio, Y. A. Lau, H. A. Khatib, J.A. Zink, N. M. Khashab and J. F. Stoddart, *Nanoscale,* 2009, **1**, 16-39.
20. Y. Zhao, J. L. Vivero-Escoto, I. I. Slowing, BG. Trewyn and V. S. Y. Lin, *Expert Opin Drug Deliv*., 2010, **7**, 1013-1029.
21. I. I . Slowing, J. L. Vivero-Escoto, C. W. Wu and V. S. Lin, *Adv. Drug. Deliv.,* 2008, **60**,1278-1288.
22. B. G. Trewyn, C. M. Whitman and V.S. Y. Lin, *Nano Lett*., 2004, **4**, 2139-*2143*.
23. N. E. Botterhuis, Q. Sun, P. C. Maqusin, R. A. van Santen and N. A. Sommerdijk, *Chem. Europ. J*., 2006, **12**, 1448-1456.
24. J. F.Chen, H. M. Ding, J. X. Wang and L. Shao, *Biomaterials,* 2004, **25**, 723-727.
25. Y. Zhu, J. Shi, H. Chen, W. Shen and X. Dong, *Micropor Mesopor Mat.,* 2005, **84**, 218-222.
26. R. Gordon, D. Losic, M. A. Tiffany, S. S. Nagy and F. A. S. Sterrenburg, *J. Trends Biotechnol*., 2008, **27**, 116-127.
27. D. Losic, J. G. Mitchell, and N. H. Voelcker, *Adv. Mater*., 2009, **21**, 2947–2958.

28. F. Noll, M. Sumper and N. Hampp, *Nano Lett* ., 2002, **2**, 91-95.
29. B. Chauhan, S. Shimpi and A. Paradkar, *Eur. J. Pharm Sci*., 2005, **26**, 219-230.
30. A. A. Ambike, K. R. Mahadik and A. Paradkar, *Pharm Res*., 2005, **22**, 990-998.
31. H. Barthel, L. Rosch, J. Weis, Fumed silica: production, properties, and applications, in: N. Auner, J. Weis (Eds.), Organosilicon Chemistry II: From Molecules to Materials, VCH Publishers, Weinheim, 1996.
32. S. Spomenka, N. Ghouchi-Eskandar, A. W. Moom Sinn, L. Dusan and A. Clive, *Curr. Drug. Discov. Technol.,* 2011, **8**, 250-268.
33. C. Nacken, M. Sameti, C. M. Lehr and H. Schmidt, *Mater. Sci. Eng.* 2003, **C23**, 93-97.
34. C. Kneuer, M. Sameti, E. G. Haltner, T. Schiestel, H. Schirra, H. Schmidt and C. M. Lehr, *Int. J. Pharm*. 2000, **196**, 257-261.
35. Z. Chen, F.C. Hsu, D. Battigelli and H. C. Chang, *Anal. Chim. Acta*., 2006, **569**, 76-82.
36. B. Fong and P. S. Russo, *Langmuir*, 1999, **15**, 4421-4426.
37. B. Fong, S. Turksen, P. S. Russo and W. Stryjewski, *Langmuir*, 2004, **20**, 266-269.
38. M. Yamaura, R. L. Camilo, M. A. Macêdo, M. Nakamura and H. E. Toma, *J. Magn. Magn. Mater.,* 2004, **279**, 210–217.
39. A. P. Taylor, R. I. Webb, J C. Barry, H. Hosmer, RJ. Gould and B J. Wood, *J. Microsc.,* 2000, **199**, 56–67.
40. A. Rezania, R. Johnson, A. R. Lefkow and K. E. Healy, *Langmuir,* 1999, **15**, 6931–6939.
41. Z. Liu, Z. Li, H. Zhou, G. Wei, Y. Song and L. Wang, *J. Microsc.,* 2005, **218**, 233–239.
42. G. F. Paciotti. *Drug Deliv*., 2004, **11**, 169–183.
43. U. Heinz, K. Hegetschweiler, P. Acklin, B. Faller, R. Lattmann and H. P. Schnebli, *Angew. Chem. Int. Ed*. 1999, **38**, 2568-2571.
44. L. P. H. Yang, S. J. Keam and G. M. Keating, *Drugs,* 2007, **67**, 2211-2230.
45. S. Steinhauser, U. Heinz, M. Bartholomä, T. Weyhermüller, H. Nick and K. Hegetschweiler,. *Eur J. Inorg. Chem*., 2004, **2004**, 4177-4192.
46. A. Shokooh Saljooghi and S. Fatemi, *Biometals*, 2010, **23**, 707-712.
47. A. Shokooh Saljooghi and S. Fatemi, *J. Appl. Toxicol.*, 2011, **31**, 139-143.
48. M. Whitnall, J. Howard, P. Ponka and D. R. Richardson, *Proc. Natl Acad Sci*., 2006, **103**, 14901–14906.
49. R. Lattmann and P. Acklin, (Novartis Pharma AG), PCT Int. Appl. WO 9749395 A1 1997, [Chem. Abstr. 1998, **128**, 114953e].
50. Y. I. Ryabukhin, L. N. Faleeva and V. G. Korobkova, *Chem. Heter. Com.,* 1983, **19**, 332-336.
51. F. Silva, F. Marques, I. C. Santos, A. Paulo, A. S. Rodrigues, J. Rueff and I. Santos, *J. Inorg. Biochem*., 2010, **104**, 523–532.
52. Y. K. Buchman, E. Lellouche, S. Zigdon, M. Bechor, S. Michaeli, and J-P (M) Lellouche, *Bioconjugate Chem*., 2013, **24**, 2076–2087.
53. R. K. Narla, Y. Dong, O. J. D'Cruz, C. Navara and F. M. Uckun, *Clin. Cancer Res*., 2000, **6**, 1546–1556.
54. D. M. Zhu, R. K. Narla, W. H. Fang, N. C. Chia and F. M. Uckun, Clin. Cancer Res., 1998, **4**, 2967–2976.
55. H. Liu, F. Zhao, R. Yang, M. Wang, M. Zheng, Y. Zhao, X. Zhang, F. Qiu, H. Wang, *Phytochemistry,* 2009, **70,** 773–778.
56. G. Y. L. Lui, P. Obeidy, S. J. Ford, C. Tselepis, D. M. Sharp, P. J. Jansson, D. S. Kalinowski, Z. Kovacevic, D. B. Lovejoy, and D. R. Richardson, *Mol. Pharmacol*., 2013, **83**, 179-190.
57. M. R. Bedford, S. J. Ford, R. D. Horniblow, T. H. Iqbal and C. Tselepis, *J. Clin. Pharmacol*., 2013, **53**, 885-891.
58. Food and Drug Administration (2015) Waiver of in vivo bioavailability and bioequivalence studies for immediaterelease solid oral dosage forms based on a biopharmaceutics classification system: guidance for industry. Food and Drug Administation Rockville, MD. http://www.fda.gov/downloads/drugs/guidancecomplianceregulatoryinformation/guidances/ucm070246.pdf. Accessed 12th June 2015
59. Novartis (2015) https://www.pharma.us.novartis.com/product/pi/pdf/exjade.pdf Accessed 12th June 2015
60. B. Chauhan, S. Shimpi, A. Paradkar, Europ. J. Pharm. Sci., 2005, **26**, 119-239.
61. A. A. Ambike, K. R. Mahadik, A. Paradkar, Pharm. Res. 2005, **22**, 990-998.
62. D. Luo, W. M. Saltzman, Nat. Biotechnol., 2000, **18**, 893-895


 

Table of Content



1. Text

   Fumed silica nanoparticles loaded with deferasirox are three and five times more cytotoxic than cisplatin and deferasirox against MDA-MB-23, respectively.

2. GRAPHIC